

Catalysis Science & Technology

Accepted Manuscript



This is an *Accepted Manuscript*, which has been through the Royal Society of Chemistry peer review process and has been accepted for publication.

Accepted Manuscripts are published online shortly after acceptance, before technical editing, formatting and proof reading. Using this free service, authors can make their results available to the community, in citable form, before we publish the edited article. We will replace this *Accepted Manuscript* with the edited and formatted *Advance Article* as soon as it is available.

You can find more information about *Accepted Manuscripts* in the [Information for Authors](#).

Please note that technical editing may introduce minor changes to the text and/or graphics, which may alter content. The journal's standard [Terms & Conditions](#) and the [Ethical guidelines](#) still apply. In no event shall the Royal Society of Chemistry be held responsible for any errors or omissions in this *Accepted Manuscript* or any consequences arising from the use of any information it contains.

Ag-loaded zeolites Y and USY as the catalysts for selective ammonia oxidation

Kinga Góra-Marek ^{a*}, Karolina A. Tarach ^a, Zofia Piwowarska ^a, Marek Łaniecki ^b, Lucjan Chmielarz ^a

^aFaculty of Chemistry, Jagiellonian University in Kraków, 3 Ingarden St., 30-060 Kraków, Poland

^bFaculty of Chemistry, A. Mickiewicz University, Poznań, Poland

corresponding authors: Kinga Góra-Marek: kinga.goramarek@gmail.com

phone:+48 12 663 20 81

Abstract

The IR spectroscopic studies of NH₃ and CO adsorption were applied to establish the status of Ag⁰ and Ag⁺ in silver loaded zeolites Y and USY. The nature of silver particles and ions and their dispersion were found to be influenced by the type of support. Application of zeolite USY as support allowed to operate such catalyst at low temperatures with high selectivity to nitrogen (95 %). Zeolite USY as support guaranteed high concentration of uniformly dispersed metallic silver species and Ag⁺ cations of strong electron acceptor properties. The silver species of defined nature together with highly acidic centres in AgUSY protected NH₄⁺ ions against oxidation thus high selectivity to nitrogen was observed.

Keywords: silver; zeolite; IR spectroscopy; NH₃-SCO

1. Introduction

Selective catalytic oxidation of ammonia is an efficient method to abate ammonia pollution. The application areas for NH_3 -SCO include for instance the treatment of waste gases from chemical production processes, ammonia slip from the NH_3 -SCR process and gasification of biomass [1-4]. Different NH_3 oxidation pathways have been recognized due to the variety of the type of catalyst used and operation conditions. Noble metals, such as Pt and Ir have been found to be highly active at low temperature for this reaction but their rapid deactivation with time has been also confirmed. Nitrogen and water vapour independently on the kind of noble metal and reaction conditions are desired products of NH_3 -SCO. However significant amounts of nitrous oxide N_2O or nitric oxide NO can be produced as well. Different types of catalytic supports, e.g. Al_2O_3 , TiO_2 or SiO_2 , were used for deposition of active noble metal phase [5-7]. The Pt/ Al_2O_3 catalysts have been reported to be the most active in NH_3 oxidation process, however with these catalysts low selectivity to nitrogen was observed. Palladium deposited on HUSY zeolite has appeared to be the most promising noble metal based catalyst, which combined high activity and selectivity in a broad temperature window [8]. Significant efficiency of these catalysts is possibly related to high dispersion of palladium species on the zeolite surface and high acidity of HUSY zeolite. Acid sites of high strength are responsible for ammonia accumulation on the catalyst surface, thus its protection against unselected oxidation.

Silver-exchanged zeolites have been extensively studied since the 1970s because of their promising catalytic properties [9-11]. The extreme activity of silver in the selective oxidation of ammonia has been previously studied by Gang et al. [12]. They compared catalytic activity of powder silver and silver deposited on silica and alumina in the process of low temperature selective ammonia oxidation. In a group of the silver-based catalysts, the highest activity was reported for Ag/ Al_2O_3 pre-treated with hydrogen. Complete ammonia oxidation with N_2 selectivity of about 82% was obtained for these catalysts operating at 160 °C. Ammonia oxidation activity of the silver-based catalysts at low temperature was found to be dependent on the catalyst ability to dissociative or non-dissociative

adsorption of oxygen [12]. Several types of oxygen species have been recognized on silver surfaces: adsorbed molecular oxygen, adsorbed atomic oxygen, subsurface oxygen and bulk dissolved oxygen. The surface coverage by these oxygen species is one of the factors ruling the selectivity to N_2 , N_2O , and NO . The adsorbed NO and N_2O species reduce the surface oxygen coverage acting as the inhibitors for NH_3 - SCO process. The selectivity to dinitrogen is improved with the increasing surface concentration of these adsorbed species.

This work was attempted in order to elucidate the influence of silver site speciation in conventional zeolite Y and its USY analogue on their activity in the NH_3 - SCO process.

2. Experimental Section

2.1. Catalyst preparation

The ammonium forms of zeolites NaY (Si/Al=2.5, CBV 100 Zeolyst, Inc.) were obtained by six fold treatment with 0.2 M NH_4NO_3 at 60 °C for 24 hours. The $\text{Na}^+/\text{NH}_4^+$ exchange degree of 80 % ($\text{Na}_{11}(\text{NH}_4)_{44}[(\text{SiO}_2)_{137}(\text{AlO}_2)_{55}]$) was confirmed by the ICP analysis. Zeolite NH_4USY (Si/Al=2.6; ($\text{Na}_5(\text{NH}_4)_{48}[(\text{SiO}_2)_{139}(\text{AlO}_2)_{53}]$) was purchased from Zeolyst Company (CBV 500). The NH_4 -form of zeolites were transformed into H-forms by calcination at 400 °C (NH_4Y) and 500 °C (NH_4USY) for 4 h. The resulting sample was denoted as HY and HUSY.

Both HY as well as HUSY were transformed to Ag-forms by the standard four-fold ion-exchange procedure. The mixture of 100 cm^3 0.2 M AgNO_3 and 1.0 g zeolite was stirred at 60 °C for 24 h. After the ion-exchange procedure was completed the samples were washed with distilled water and dried at 100 °C. The Ag content of resulting materials were characterized by ICP method (Table 1).

Table 1. The composition of Ag-exchanged zeolites.

Samples	Si/Al	Ag/Al	Formula
HY	2.5	-	$\text{Na}_{11}\text{H}_{44}[(\text{SiO}_2)_{137}(\text{AlO}_2)_{55}]$
AgY	2.5	0.49	$\text{Ag}_{27}\text{Na}_5\text{H}_{23}[(\text{SiO}_2)_{137}(\text{AlO}_2)_{55}]$
HUSY	2.6	-	$\text{Na}_5\text{H}_{48}[(\text{SiO}_2)_{139}(\text{AlO}_2)_{53}]$
AgUSY	2.6	0.51	$\text{Ag}_{27}\text{Na}_4\text{H}_{22}[(\text{SiO}_2)_{139}(\text{AlO}_2)_{53}]$

2.2. Characterization methods

2.2.1. Structural and textural parameters

The X-ray diffraction (XRD) patterns of the samples were recorded with a D2 Phaser diffractometer (Bruker) using $\text{Cu K}\alpha$ radiation ($\lambda = 1.54060 \text{ \AA}$, 30 kV, 10 mA).

The BET surface area and pore volume of the samples were determined by N_2 sorption at -196 °C using a 3Flex (Micromeritics) automated gas adsorption system. Prior to the analysis, the samples

were degassed under vacuum at 250 °C for 24 h. The specific surface area (S_{BET}) was determined using BET (Brunauer-Emmett-Teller) model according to Rouquerol recommendations [13]. The micropore volume and specific surface area of micropores were calculated using the Harkins-Jura model (t -plot analysis).

The micrographs were obtained using transmission electron microscope (JEOL 2100F) working at 200 KV, with Field Emission Gun (FEG), EDX analysis and STEM detectors for bright and dark mode.

2.2.2. IR spectroscopy studies with probe molecules

Prior to FTIR studies, the zeolite samples were pressed into the form of self-supporting wafers (ca. 5 mg/cm²) and in situ thermally treated in an IR cell at 450 °C under vacuum for 30 min. Then, the samples were cooled down to 200 °C and contacted with hydrogen. Reduction was performed at 200 °C for 30 minutes. After this time, the samples were evacuated at 450 °C for 1 hour cooled down to room temperature.

Ammonia (PRAXAIR, 3.6), nitrogen monoxide (Linde Gas Poland 99.5%) and carbon monoxide (Linde Gas Poland, 3.7) were used as probe molecules.

Spectra were recorded with a Bruker Tensor 27 spectrometer equipped with an MCT detector. The spectral resolution was of 2 cm⁻¹.

2.2.3. TPR studies

After sample (50 mg) stabilization in stream of Ar at 30°C the temperature increased to 450°C with the rate of 5°C min⁻¹ and pulsed injections of hydrogen were sent to the reactor every 25 seconds using a constant flow rate of 30 cm³ min⁻¹ of 1 vol. % of H₂ diluted in Ar. The reduction was maintained for 1 hour at the final temperature. A magnesium perchlorate water trap was used to remove water from the outlet gas stream. The hydrogen consumption was monitored by a thermal conductivity detector (TCD).

2.2.3. XPS Measurements

The surface chemical composition of the samples was studied by XPS in an ultrahigh vacuum (UHV). Prior to the measurements, all the samples were evacuated in the pre-treatment chamber at a pressure lower than 10^{-7} kPa, heating slowly from room temperature to 300 °C. In order to remove water and other adsorbed species the temperature was kept constant during 30 min. The X-ray photoelectron spectra (XPS) were measured on a Prevac photoelectron spectrometer equipped with a hemispherical VG SCIENTA R3000 analyser. The photoelectron spectra were measured using a monochromatized aluminium Al K α source ($E = 1486.6$ eV) and a low-energy electron flood gun (FS40A-PS) to compensate the charge on the surface of nonconductive samples. The base pressure in the analysis chamber during the measurements was $5 \cdot 10^{-9}$ mbar. Spectra were recorded with constant pass energy of 100 eV for the survey and for high-resolution spectra. The binding energy scale was referenced to the Au 4f $_{7/2}$ peak (84,0 eV) of a clean gold. The composition and chemical surrounding of the sample surface were investigated on the basis of the areas and binding energies of Pd 3d, Al 2p, Si 2p and O 1s photoelectron peaks. The binding energy (BE) of core-levels O 1s, Si 2p, Al 2p, and Ag 3d was measured. The Si 2p peak at 102.3 ± 0.1 eV binding energy was taken as an internal reference.

2.3. Catalytic tests

Ag-exchanged zeolites were tested as catalysts for the selective catalytic oxidation of ammonia (NH₃-SCO). The experiments were performed under atmospheric pressure in a fixed-bed flow microreactor system (i.d., 7 mm; l., 240 mm). The reactant concentrations were continuously monitored using a quadrupole mass spectrometer RGA 200 (PREVAC) connected to the reactor via a heated line. Before the reaction, the catalyst sample (50 mg diluted with 50 mg of SiO₂ (POCH, BET 192 m²g⁻¹, particle size of 120-355 μ m)) was outgassed in a flow of pure helium at constant heating rate of 10 °C min⁻¹ up to 450 °C and then cooled down to room temperature. The composition of the gas mixture at the reactor inlet was [NH₃] = 0.5 vol. %, [O₂] = 2.5 vol. % and [He] = 97 vol. %. Total flow rate of the

reaction mixture was $40 \text{ cm}^3 \text{ min}^{-1}$, while a space velocity was about $15,400 \text{ h}^{-1}$. The reaction was studied at temperatures ranging from 100 to 500 °C with the linear temperature increase of 10 °C min^{-1} . For the selected catalyst AgUSY, additional catalytic tests with the gas mixture containing water vapour or carbon dioxide were performed. In these cases, the reaction mixtures with the following compositions were used: $[\text{NH}_3] = 0.5 \text{ vol.}\%$, $[\text{O}_2] = 2.5 \text{ vol.}\%$, $[\text{H}_2\text{O}] = 3.2 \text{ vol.}\%$, $[\text{He}] = 93.8 \text{ vol.}\%$ or $[\text{NH}_3] = 0.5 \text{ vol.}\%$, $[\text{O}_2] = 2.5 \text{ vol.}\%$, $[\text{CO}_2] = 4.8 \text{ vol.}\%$, $[\text{He}] = 92.2 \text{ vol.}\%$.

The signal of the helium line served as an internal standard to compensate possible fluctuations of the operating pressure. The sensitivity factors of analysed lines were calibrated using commercial mixtures of gases.

3. Results and Discussion

3.1. Structural and textural characteristics

The presence of reflections typical of the FAU structure in diffractograms of H-zeolites (Fig. 1) indicates that their calcination at 400 °C did not disturb the zeolitic structure. Additionally, the almost identical intensity of the reflections comparing to H-zeolite, point to the preservation of the FAU structure also after ion-exchange procedure. The reflections typical of silver species were not identified in the diffractograms of AgY and AgUSY indicating that silver clusters are of a small crystallite size and/or of amorphous nature. Most likely their growth is restricted by the pore size of zeolite Y.

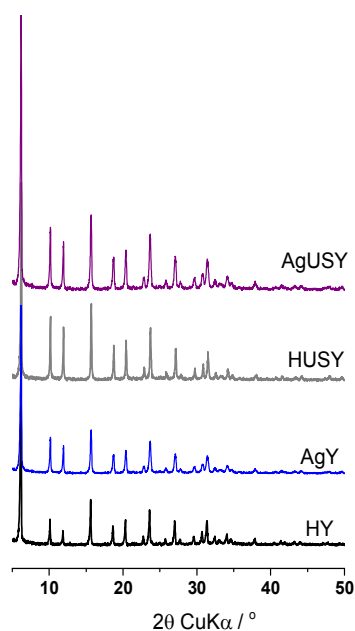


Figure 1. X-ray diffraction patterns.

Table 2. Chemical analysis and textural parameters of the studied H- and Ag-zeolites. Average size of Ag particle (\varnothing) in nm derived from STEM studies.

Samples	$S_{\text{BET}} / \text{m}^2 \text{g}^{-1}$	$S_{\text{micro}} / \text{m}^2 \text{g}^{-1}$	$V_{\text{micro}} / \text{cm}^3 \text{g}^{-1}$	\varnothing / nm
HY	890	800	0.29	-
AgY	698	399	0.19	7-14 (62)*
HUSY	1037	942	0.36	-
AgUSY	901	758	0.30	5-7 (87)*

*x % of the total population of Ag particles

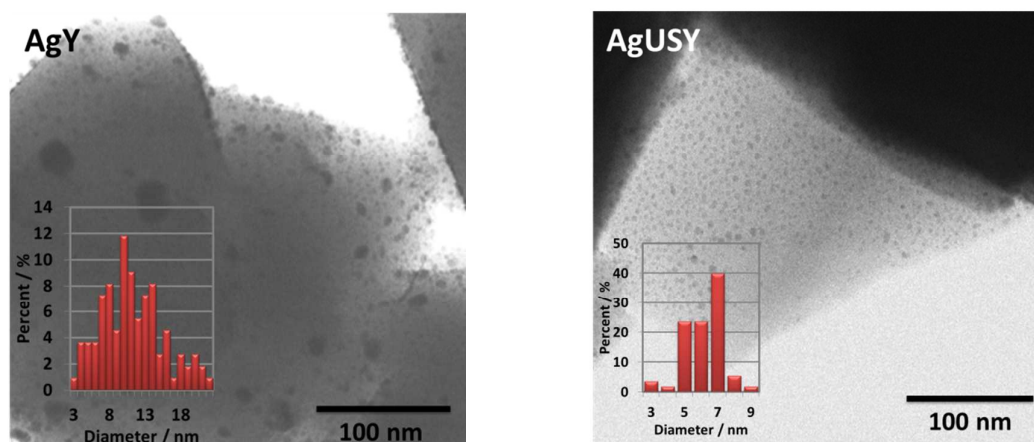


Figure 2. STEM micrographes and Ag-particles size distribution of studied Ag-exchanged zeolites.

The textural parameters of the studied catalysts were affected by the presence of silver species (Table 2). Surface area and pore volume of AgY zeolite were considerably reduced, what indicates that part of Ag clusters was located in micropores. For ultrastable zeolite AgUSY the micropore volume was less affected by metal deposition due to the presence of the secondary system of mesopores providing better metal dispersion. Moreover, the analysis of STEM micrographes (Fig. 2) as well as of the size of Ag-particles (derived also from STEM studies, Table 1) confirmed that in the case of the HUSY support better dispersion of metal clusters was achieved. Indeed, the acidic properties of the support have been reported to be the most important factors determining the metal phase dispersion and modifying the metallic phase to make it more electron deficient [14, 15]. Thus higher Brønsted and Lewis acidity of the HUSY support seems to be beneficial to more uniform metal phase dispersion.

3.2. Acidic properties

Both size and arrangement of pores are the crucial factors influencing the specific sorption properties of zeolites. However, well documented involvement of acid sites, mainly Brønsted type, in many redox reactions clearly evidences that applicability of zeolites as supports is ruled by their acidic properties. Among many methods allowing for detailed characterization of acidity of solids the IR quantitative studies of the acid sites speciation are the most as common as important. In the present work ammonia molecule, one of the reagents in the NH_3 -SCO process, was employed as probe. Interaction of ammonia with Brønsted and Lewis acid sites resulted in development of the 1450-1445 cm^{-1} band of NH_4^+ ammonium ions and the 1620 cm^{-1} band attributed to ammonia coordinatively bonded to Lewis acid sites [16]. The concentrations of both Brønsted (NH_4^+) and Lewis (NH_3 -L) acid sites were calculated from the maximum intensities of the NH_4^+ and NH_3 -L bands (Fig. SI.1) and the corresponding values of the extinction coefficients: 0.11 $\text{cm}^2 \mu\text{mol}^{-1}$ and 0.026 $\text{cm}^2 \mu\text{mol}^{-1}$ for the NH_4^+ and the NH_3 -L band, respectively [17, 18]. The comparison of the concentrations of the Brønsted and Lewis acid sites in H- and Ag-zeolites determined by an IR quantitative measurements is given in Table 3. Deposition of Ag species in zeolites HY and HUSY resulted in a decrease of the protonic sites concentration with the simultaneous increase of the electron acceptor site amount. However, for both zeolites the number of Ag species considered as newly created Lewis sites (L_{Ag}) and expressed as $L_{\text{AgY}} - L_{\text{HY}}$ and $L_{\text{AgUSY}} - L_{\text{HUSY}}$ is noticeably lower than the concentration of Ag calculated from chemical analysis (Table 3). Such discrepancy can originate from the presence of clustered forms of silver species both oxide silver species and/or silver cationic clusters $[\text{Ag}_n]^{x+}$. The latter species originate from the photoreduction of Ag(I) species when the Ag-samples are exposed to the light [19]. The electrons required for the autoreduction process originate from oxygen atoms of the zeolite framework or from the oxidation of hydration water to oxygen [10, 20, 22]. The amounts of Ag moieties detected by ammonia chemisorption do not differ significantly for both Ag-zeolites. Indeed, in zeolite AgY silver cations Ag^+ , clusters $[\text{Ag}_n]^{x+}$ (e.g. Ag_3^+ ; Ag_3^{2+} ; Ag_3^{3+}) as well as metallic Ag^0 species are located in the sodalite cages and hexagonal prisms, thus their accessibility to

NH₃ molecule is limited [22]. These structure constraints are not applied to the AgUSY, thus the silver moieties should be more accessible to ammonia molecules. However, the accessibility of NH₃ molecules to Ag moieties is comparable for both USY and Y zeolite, though different structural characteristic and dispersion of silver sites. According to STEM data the dispersion of Ag species in AgY is less uniform: high population of small 3-8 nm particles (20 %) is followed by the presence of highly aggregated 7-14 nm Ag clusters (62 %). On the other hand, the STEM micrograph recorded for AgUSY clearly demonstrates the homogenous dispersion of 5-7 nm silver particles in the zeolite matrix (Table 2, Figure 2).

Information on the acid strength of Brønsted and Lewis acid sites was derived from ammonia thermodesorption experiments followed by IR spectroscopy. The intensities of the diagnostic bands upon the desorption at 400 °C and 200 °C were defined as A_{400} and A_{200} for each kind of acid sites, respectively. The A_{400}/A_{200} ratios, determined for both of Brønsted (NH₄⁺ ions band at 1450 cm⁻¹) and Lewis (NH₃-Lewis adducts band at 1620 cm⁻¹) acid sites, express the fraction of ammonia molecules resisted against the desorption at 400 °C. The A_{400}/A_{200} values (Table 3) were taken as the measure of the acid strength of protonic and electron acceptor sites in studied catalysts. It is well seen that the strength of acid sites in zeolite HUSY is significantly enhanced. It is not surprising because the presence of extraframework aluminum species EFAl possessing high electron acceptor properties themselves is also responsible for noticeable Brønsted acidity enhancement. Besides, dealumination of the framework resulting in lower framework Si/Al ratio guarantees higher strength of the Si(OH)Al groups. In Ag-exchanged zeolite Y the strength of the acid sites increases what can be correlated with the appearance of new electron acceptor Ag⁺ sites. In zeolite AgUSY the Lewis site strength remains on the same level suggesting that newly formed cationic sites are of the same electron acceptor properties as those existing in the form of EFAl moieties. It has previously been reported [12] that the kind of support plays a crucial role in activity and selectivity of silver-based materials. Especially the alumina-supported silver catalyst showed high selectivity and activity for ammonia oxidation to nitrogen at very low temperature compared with silica-supported silver catalyst and silver powder

catalyst. The 10 wt.%Ag/Al₂O₃ catalytic performance was related to the specific interaction of silver with alumina support. The extraframework aluminum species EFAl of high electron acceptor properties were found also in zeolite AgUSY, thus this catalyst is supposed to be more active and selective to nitrogen than EFAl-poor zeolite AgY.

Table 3. Concentration (in $\mu\text{mol g}^{-1}$) of silver in the zeolite samples determined by ICP method as well as concentrations and acid strength of Brønsted (B) and Lewis (L) sites.

Samples	B $\mu\text{mol g}^{-1}$	L $\mu\text{mol g}^{-1}$	Acid strength		Ag _{ICP} $\mu\text{mol g}^{-1}$	L _{Ag} L _{Ag-zeolite} - L _{H-zeolite} $\mu\text{mol g}^{-1}$
			A_{400}/A_{200}			
			B	L		
HY	1850	954	0.35	0.15	-	-
AgY	1198	1605	0.55	0.35	1952	651
HUSY	895	1085	0.74	0.89	-	-
AgUSY	504	1895	0.81	0.85	1975	810

3.3. Status of silver sites in the catalysts

It is widely known that zeolite HUSY can be considered as a mixture of crystalline zeolite structure and the highly dispersed EFAl extraframework alumina species. For this reason mesoporous structure of zeolite HUSY guarantees the presence of Brønsted and Lewis acid sites in large quantity and high acid strength. Specific textural and acidic properties of HUSY influence both the dispersion and electron acceptor properties of Ag moieties. In this work the silver speciation was followed by H₂-TPR, XPS, and IR spectroscopy studies to evidence the difference in the properties of Ag moieties dispersed in zeolites HY and HUSY.

3.3.1. H₂-TPR

H₂-TPR profiles of AgY and AgUSY zeolites are shown in Fig. 3. The reduction of silver species in faujasites was followed up to about 500 °C. The peaks in the temperature region of 156-220 °C can be tentatively ascribed to highly dispersed Ag₂O and the silver cationic clusters Ag_n⁺ formed by the reaction between metallic Ag⁰ species and Ag⁺ exchangeable cations [23, 24]. The high temperature

peaks at 340 °C and 410 °C originate from further reduction of the Ag_n^+ to metallic silver Ag^0 [25-27]. The lack of peak at 340 °C in the H_2 -TPR profile of AgUSY is related to the higher resistance of Ag_n^+ species against reduction. It was reported [27] that high concentration of Brønsted acid sites favours the reoxidation of Ag^0 formed in the reduction process. Thus, in the case of zeolite AgY, with a higher concentration of protonic sites, a complete reduction of Ag_n^+ occurred at lower temperature than for zeolite AgUSY, with the lower content of Brønsted acid sites.

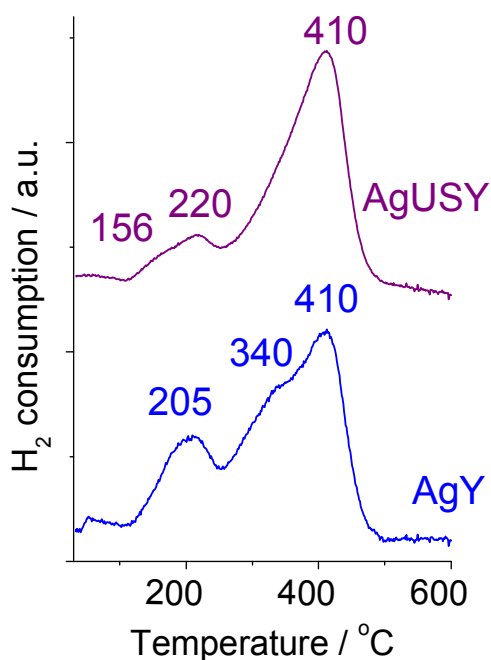


Figure 3. H_2 -TPR profiles of the studied catalysts.

3.3.1. X-ray Photoelectron Spectroscopy (XPS)

To investigate the effect of the different aluminium content in zeolites AgY and AgUSY on the chemical state and surface concentration of silver species in the catalysts, the photoelectron spectra were analysed. Ag 3d XPS regions (Fig. 4) of Ag-zeolites Y and USY are simple doublets with energy separation of ca. 6.0 eV. The Ag 3d_{5/2} binding energies equal 369.0–369.7 eV for both Ag-zeolites could be assigned to Ag^+ cations located at exchange positions [28, 29]. The additional peaks of Ag 3d at lower BE values (368.0–367.6 eV) originate from metallic species [30]. Similar values of binding

energies do not allow for the differentiation of metal moieties in studied zeolites in terms of neither their electron affinity nor their dispersion. Also the distribution of Ag species between Ag^+ and Ag^0 is somewhat difficult due to a small shift of the Ag 3d peaks typical of these species [31], nevertheless significantly larger amount of metallic silver is evidenced for AgUSY zeolite than for AgY. As mentioned above the binding energy positions of Ag 3d are not sufficient to perform the comprehensive analysis of the silver oxidation states [31], thus the speciation of Ag moieties was studied by infrared low temperature CO adsorption.

Table 4. XPS binding energy peak positions in studied Ag-zeolites.

Peak	Binding energy [eV]	
	AgY	AgUSY
$\text{Ag}^0 3d_{3/2}$	372.7	372.6
$\text{Ag}^0 3d_{5/2}$	368.0	367.7
$\text{Ag}^+ 3d_{3/2}$	374.4	374.3
$\text{Ag}^+ 3d_{5/2}$	369.7	369.0
Ag^+/Ag^0	0.79	0.54

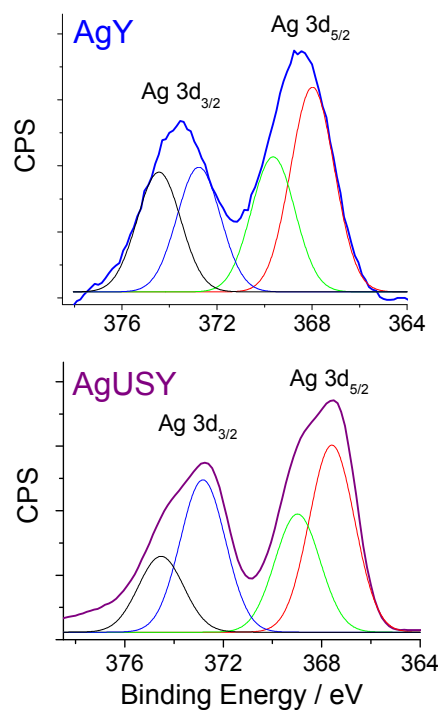


Figure 4. XPS data of zeolites AgY and AgUSY.

3.3.2. IR studies of CO sorption

IR studies of CO adsorption deliver valuable information on the state and bonding characteristics of silver ions. The spectra of CO adsorbed on AgY and AgUSY are presented in Figure 5. In AgY, two bands of $\text{Ag}^+(\text{CO})$ monocarbonyls at 2194 and 2175 cm^{-1} were observed proving the presence of two Ag^+ sites of different electron acceptor properties, the most probably resulting from the location of Ag^+ in S_{II} sites (the monocarbonyl band settled at 2175 cm^{-1}) and from Ag^+ of lower number of oxygen atoms in vicinity, thus possibly in the S_{III} sites (a small band at 2194 cm^{-1}). Interaction of carbon monoxide with silver sites in AgUSY led to the appearance of a strong band with the maximum settled at 2189 cm^{-1} and less intense band at 2199 cm^{-1} . Higher frequency of monocarbonyl band in AgUSY is correlated with electronegativity of framework ruled by lower concentration of AlO_4^- in the AgUSY framework [32]. This lower framework Si/Al ratio guarantees higher electron acceptor properties of Ag^+ species. It is also well-known that the partial dealumination of the zeolite framework results in the formation of extra-framework aluminium (EFAl) species that significantly enhance the acidic properties, thus catalytic activity of the zeolite [33]. Several forms of the EFAl species have been proposed in the literature: positively charged species such as Al^{3+} , AlO^+ , $\text{Al}(\text{OH})_2^+$ and AlOH^{2+} that are stabilized at specific cationic sites both in the sodalite cages and in supercages, and neutral or polymeric intrazeolitic aluminium-oxo or hydroxo species such as AlOOH , $\text{Al}(\text{OH})_3$ and Al_2O_3 [34, 35]. The association of EFAl into an amorphous silica–alumina phase has also been claimed [36]. The cationic EFAl species withdraw some negative charge of the framework oxygen atom leading to reduction of density of negative charge in next-nearest-neighbour positions. Consequently the Ag^+ cations located in the vicinity of EFAl species are less neutralized by framework and possess greater electron acceptor properties. Ligation of CO to the most electron acceptor Ag^+ cations in zeolite AgUSY leads to the formation of the $\text{Ag}^+(\text{CO})$ adducts represented by the monocarbonyl band of the highest frequency (2199 cm^{-1}).

Additionally, for both Ag-exchanged zeolites the presence of metallic silver is demonstrated by the monocarbonyls $\text{Ag}^0(\text{CO})$ band at 2160 cm^{-1} . The negligible intensity of this band is not absolute evidence for a minor amount of metallic silver species on the surface of catalysts due to a greatly reduced value of the absorption coefficient of the $\text{Ag}^0(\text{CO})$ monocarbonyl band [37]. The concentration of the silver species in studied zeolites (Table 4) were calculated on the basis of the maximum intensities of the $\text{Ag}^+(\text{CO})$ and $\text{Ag}^0(\text{CO})$ monocarbonyl bands (Fig. 4) and their absorption coefficients [37].

Table 5. Concentration of Ag^+ and Ag^0 species in studied zeolites attained from IR quantitative experiments of CO sorption and the total concentration of Ag derived from chemical analysis.

Samples	IR studies $\text{Ag} / \mu\text{mol g}^{-1}$			Chemical analysis $\text{Ag} / \mu\text{mol g}^{-1}$
	Ag^+	Ag^0	$\text{Ag}^+ + \text{Ag}^0$	
AgY	500	122	622	1952
AgUSY	270	680	950	1975

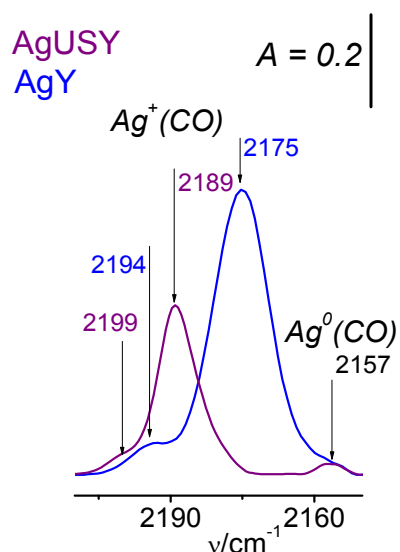


Figure 5. The maximum intensity of the $\text{Ag}^+(\text{CO})$ and $\text{Ag}^0(\text{CO})$ monocarbonyls bands in zeolites AgY and AgUSY.

Concentration of the Ag^+ cations in AgUSY is significantly reduced in comparison with AgY (Table 5) due to the formation of metallic species in large amount. As mentioned earlier the silver metallic clusters can evolve both from the photoreduction and autoredution process taking place under

vacuum treatment at high temperature. Due to the lower electronegativity of the USY zeolite framework the reduction processes were more efficient, thus bigger amount of Ag^0 was detected for zeolite AgUSY. The discrepancy between the amounts of Ag species detected by CO and derived from chemical analysis (Table 5) origins from either the presence of clustered forms of metallic silver or inaccessibility of Ag species (Ag^0 , Ag_n^+ , Ag^+) due to the structure constrains.

Summing up, besides uniform dispersion of silver clusters, the AgUSY zeolite offers the Ag^+ cationic species of much stronger electron acceptor properties than zeolite AgY.

3.4. IR studies of NH_3 transformation over zeolites studied

Saturation of all acid and redox sites with an excess of ammonia at $100\text{ }^\circ\text{C}$ was followed by 10 min evacuation at the same temperature to remove the ammonia physisorbed. In both zeolites ammonia was found to be bonded on the catalyst surface as NH_4^+ ions (1455 cm^{-1} bands) and $\text{NH}_3\text{-L}$ moieties (1610 cm^{-1} bands) (Fig. 6, spectrum a). Heating of the catalysts in oxygen atmosphere up to $150\text{ }^\circ\text{C}$ (spectrum b) for 5 min. resulted in ammonia oxidation recognized as the appearance of a series of species: N_2O (2224 cm^{-1}), N_2O_4 (1742 cm^{-1}), chemisorbed NO_2 (1678 cm^{-1}), bidentate nitrates (1578 cm^{-1}), and nitrites (1465 cm^{-1}) [38, 39]. The band at 1620 cm^{-1} originates from bridged nitrates and/or H_2O formed as the final product. No bands typical to silver nitrosyl complexes were detected due to the weak electrophilicity of the Ag^+ ions and the lack of a π -backdonation. Higher intensities of the oxidation product bands were found for AgUSY than for AgY sample, in line with higher catalytic activity of AgUSY. The nitrates and/or nitrites as well as N_2O are possible intermediates in the SCR of NO_x . Therefore, the presence of NO_3^- and/or NO_2^- suggests that that $\text{NH}_3\text{-SCO}$ proceeds *via* the *i*-SCR mechanism involving ammonia partial oxidation to nitrogen oxide, which then is reduced to N_2 and/or N_2O by ammonia unreacted. However, the elementary surface reaction steps need to be identified to justify such assumption.

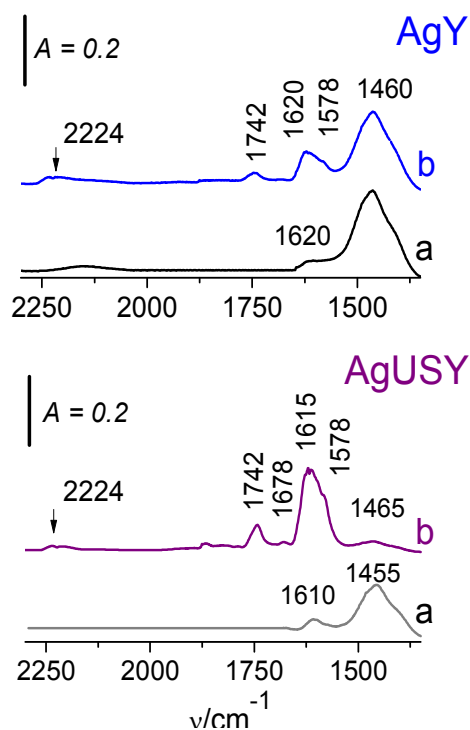


Figure 6. IR spectra recorded at RT: (a) after saturation of zeolitic active sites with NH_3 at $100\text{ }^\circ\text{C}$ (b) after introduction of O_2 (1 NH_3 : 5 O_2) and heating of the catalysts up to $150\text{ }^\circ\text{C}$ for 5 min.

3.5. Catalytic tests

Figure 7 presents the results of the catalytic tests in the process of selective ammonia oxidation. Nitrogen is a desired product of ammonia oxidation, while nitrogen oxides (NO , NO_2 and N_2O) are undesired side-products. It can be seen that for the process performed in the presence of HY and HUSY, the ammonia conversion at $500\text{ }^\circ\text{C}$ did not exceed 40 and 50%, respectively. Among the reaction products, apart from N_2 , also significant contributions of NO and N_2O were detected, especially for HUSY. Comparison of the Si/Al ratio (Table 1) and concentration of Brønsted and Lewis acid sites content (Table 3), leads to the hypothesis that not all aluminium ions form acid sites. For both HY and HUSY the Si/Al ratio is very similar (2.5 and 2.6, respectively), while for HY the total content of acidic sites ($2804\text{ }\mu\text{mol g}^{-1}$) is significantly higher than for HUSY ($1970\text{ }\mu\text{mol g}^{-1}$). In zeolite HUSY aluminium can be deposited in the form of non-acidic aggregated alumina species as well as extraframework aluminium moieties with the increased Lewis acidity. Deposition of silver species on

HY and HUSY influenced significantly the process of selective ammonia oxidation to N_2 and H_2O . It should be noted that for both Ag-catalysts the selectivity to nitrogen was about 90% at temperature as high as 250 °C. Moreover, AgUSY effectively operated at temperatures significantly lower (of about 100 °C) in comparison to the AgY catalyst and achieved the selectivity of 95 % at 175 °C. Considering the similar silver loading in both the catalysts such significant difference in their catalytic activity can be inferred not only to the amount of silver deposited but also to the different electron donor properties of silver species. Dispersion of Ag is unquestionable factor responsible for high activity and selectivity of the silver-based catalyst since well-dispersed and small particles of Ag^0 were found to enhance catalytic activity at low temperature (<140 °C), whereas large particles of Ag^0 were responsible for a high N_2 selectivity [12, 40]. For the more active AgUSY catalyst more uniform dispersion of silver species was identified by STEM. However, the average size of silver particles in AgUSY is smaller than for zeolite AgY, what could result in their higher activity. Another factor influencing both activity and selectivity of catalyst is reducibility of the silver particles. Indeed, smaller particles undergo reduction more easily than larger particles. However, the reducibility also strongly depends on the acidity of support. Silver species deposited on acidic supports were recognized to be more easily oxidized than those supported on neutral or basic support [27]. Indeed, the presence of bigger amount of Brønsted acid sites was evidenced in quantitative ammonia-sorption studies for AgY (Table 3). Also, the results of H_2 -TPR showed a higher contribution of easy-reducible silver species in case of the AgY sample while those deposited on USY underwent reduction at higher temperature. The diverse status of silver cations in zeolites AgY and AgUSY was confirmed in IR studies of CO sorption. The AgUSY zeolite ensures high concentration of Ag^+ cationic species of strong electron acceptor properties while silver cations in zeolite AgY represent weaker electron acceptor properties. Consequently, high selectivity of the AgUSY catalyst to nitrogen can be related to protection against oxidation of ammonia chemisorbed on strongly electron acceptor Ag^+ cations hosted in the zeolite framework and therefore their ability to reduce the nitrogen oxides. Zhang et al. [40] in the studies of the mechanism of selective catalytic oxidation of ammonia to nitrogen over

Ag/Al₂O₃ have evidenced that different Ag species on Ag/Al₂O₃ significantly influence O₂ uptake by catalysts; while different oxygen species affect the activity of NH₃ oxidation at low temperature. At temperatures lower than 140 °C NH₃ oxidation follows the imide (NH) mechanism while at higher temperatures oxidation proceeds according to *i*-SCR mechanism. It has been found that at lower temperatures (<140 °C) both adsorbed NH₃ and O₂ could be activated by Ag⁰ as the main active species on the Ag/Al₂O₃. At temperatures above 140 °C the Ag⁺ cations have been also considered as the species activating adsorbed ammonia molecules [40]. In our case highly electron acceptor Ag⁺ cations in AgUSY strongly bonded NH₃ molecules protecting them against oxidation. Thus the in situ produced NO_x⁻ (NO₃⁻ and/or NO₂⁻) and NO_x species interacted with the adsorbed ammonia (NH_x species) and were reduced to N₂ according to *i*-SCR mechanism.

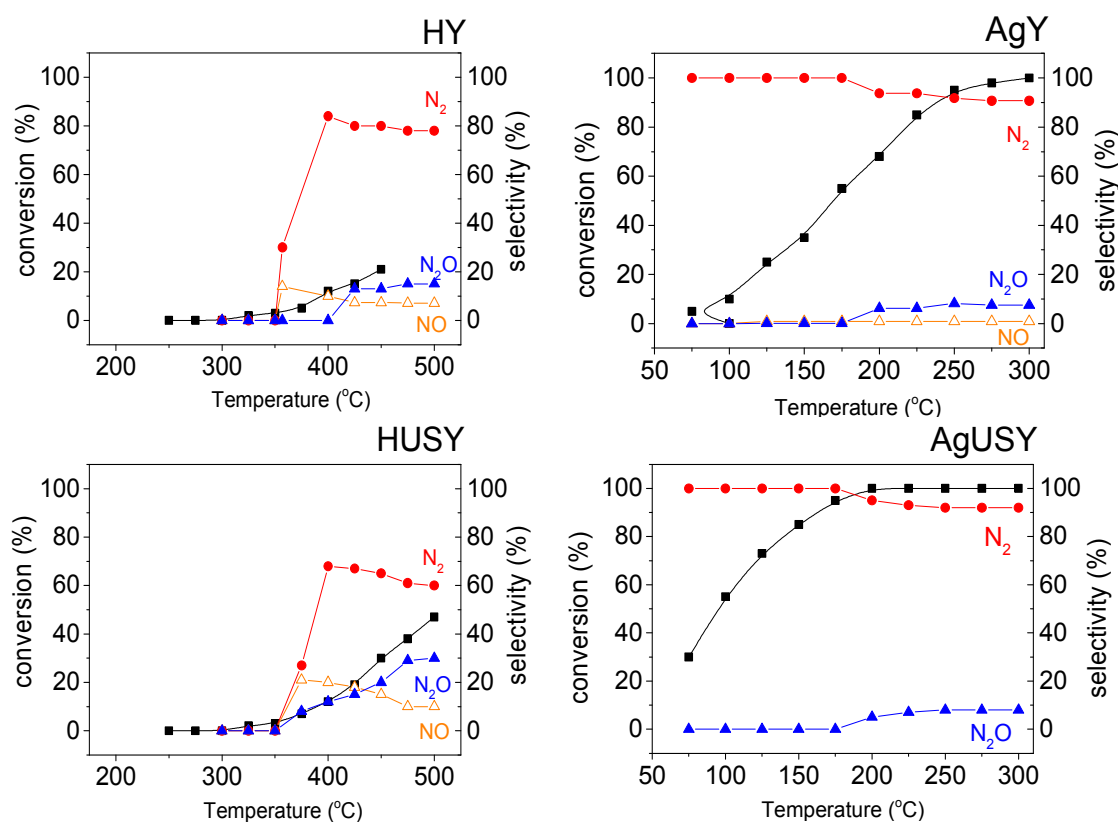


Figure 7. Results of catalytic tests in the process of selective oxidation of ammonia for H- and Ag-forms of zeolites Y and USY.

Moreover, the Brønsted and Lewis acid sites are also considered as additional reservoir of chemisorbed substrate, mainly for ammonia adsorption. Again, the stronger bonding of ammonia to acid sites, the more enhanced protection of NH_4^+ ions against oxidation and finally higher selectivity to nitrogen. Nevertheless, ammonia molecules chemisorbed on acid sites of zeolite USY and Ag^+ cations can be transported on reactive Ag^0 -species in the desorption–readsorption cycle. For the more active AgUSY catalyst acid sites possess higher acid strength than those in conventional AgY. Thus, it could be suggested that for the formulation of active and selective catalyst for ammonia oxidation both Lewis acid sites (possibly located on nanometric alumina aggregates) and well dispersed metallic silver clusters as well as strongly electron acceptor Ag^+ cations have to coexist. Gang et al. [12] revealed that the NH_3 oxidation over the Ag-based catalysts followed the *i*-SCR mechanism. Probably also in the case of zeolite AgUSY the ammonia oxidation proceeds according (*i*-SCR) and high selectivity of the AgUSY catalyst to nitrogen, especially in the high temperature range, is related to protection of ammonia chemisorbed on the Brønsted acid sites against oxidation and therefore its ability to reduce the nitrogen oxides.

For the AgUSY catalyst activity tests with the gas mixture containing water vapour or carbon dioxide were carried out. An introduction of water vapour into the reaction mixture only slightly decreases ammonia conversion (Fig. 8). Additionally, the comparison of selectivities obtained for the process performed in dry and wet (Fig. 8) conditions evidences that ammonia is more selectively oxidized to N_2 when water vapour was introduced into the gas mixture. Similar results were obtained for test performed with the reaction mixture containing CO_2 . It is clearly shown that carbon dioxide plays a role of inert gas under reaction conditions and therefore, both NH_3 conversion as well as selectivity to N_2 are very similar to the results obtained for the standard reaction mixture.

For AgUSY catalyst additional long-term stability test in the presence of water vapour was done. It can be seen that during the whole period of time of the test ammonia conversion was nearly constant maintaining the level of 93-96% . Thus, it could be conclude that the studied catalyst presents relatively high stability under reaction conditions.

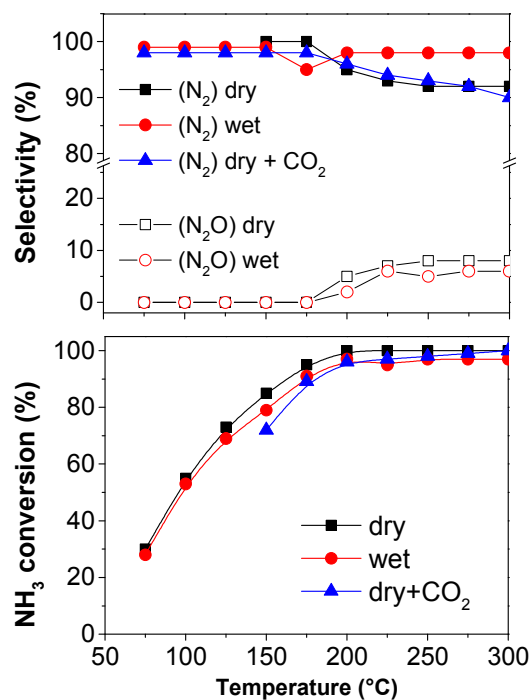


Figure 8. The results of catalytic tests performed in wet atmosphere or reaction mixture containing CO₂ for AgUSY. For comparison also results obtained in tests performed in the absence of H₂O and CO₂ are shown.

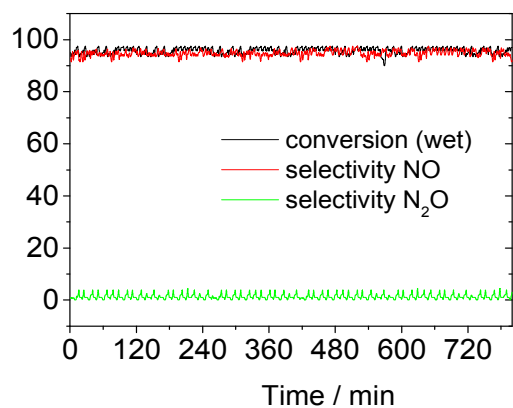


Figure 9. Stability tests performed for AgUSY in the presence of water vapour.

4. Conclusions

The AgY and AgUSY catalysts showed high selectivity to nitrogen (90%) at temperature as high as 250 °C, however zeolite AgUSY effectively operated with selectivity of 95% to nitrogen at 175 °C. Both the uniform dispersion of metallic silver species and the electron acceptor properties of Ag⁺ cations were found to be the key factors that influenced the activity and N₂ selectivity of the catalysts in the process of selective ammonia oxidation. Finally, zeolite USY as support guaranteed high concentration of both uniformly dispersed metallic silver and high concentration of Ag⁺ cations of strong electron acceptor properties. Together with acid centres of high strength all these features provided enhanced protection of NH₄⁺ ions against oxidation and finally higher selectivity to nitrogen.

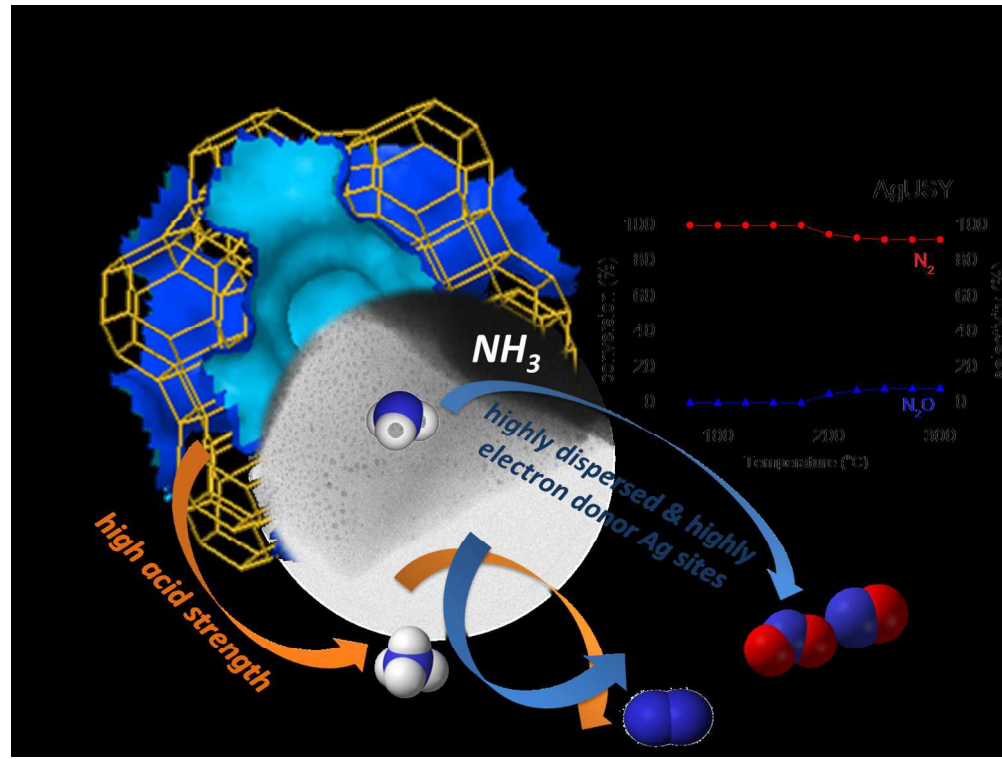
Acknowledgement

This work was financed by Grant No. 2013/09/B/ST5/00066 from the National Science Centre, Poland.

References

1. S. Shrestha, M.P. Harold, K. Kamasamudram, A. Yezerets, *Top. Catal.* 56 (2013) 182–186.
2. A.Y. Stakheev, D.A. Bokarev, A.I. Mytareva, R.K. Parsapur, P. Selvam, *Mendeleev, Commun.* 24 (2014) 313–315.
3. R. Burch, B.W.L. Southward, *Chem. Commun.* 8 (2000) 703–704.
4. R. Burch, B.W.L. Southward, *J. Catal.* 195 (2000) 217–226.
5. A. Scheuer, W. Hauptmann, A. Drochner, J. Gieshoff, H. Vogel, M. Votsmeier, *Appl. Catal. B: Environmen.* 111–112 (2012) 445–455.
6. Y. Li, J.N. Armor, *Appl. Catal. B: Environmen.* 13, (1997) 131–139.
7. A. Scheuer, M. Votsmeier, A. Schuler, J. Gieshoff, A. Drochner and H. Vogel, *Top. Catal.*, 52 (2009) 1847–1851.
8. M. Jabłonska, A. Krol, E. Kukulska-Zajac, K. Tarach, L. Chmielarz, K. Góra-Marek, *J. Catal.*, 2014, 316, 36–46.
9. P.A. Jacobs, J. B. Uytterhoeven, H.K. Beyer, *J. Chem. Soc., Chem. Commun.* (1977) 128.
10. P. A. Jacobs, J. B. Uytterhoeven, *J. Chem. Soc., Faraday Trans.* 75 (1979) 56–64.
11. J. Howard, T.C. Waddington, C.J. Wright, *J. Chem. Soc., Chem. Commun.* (1975) 775.
12. L. Gang, B. G. Anderson, J. van Grondelle R. A. van Santen, *Appl. Catal. B: Environmen.* 40 (2003) 101–110.
13. J. Rouquerol, P. Llewellyn, F. Rouquerol, *Stud. Surf. Sci. Catal.* 160 (2007) 49–56.
14. K. Okumura, S. Matsumoto, N. Nishiaki, M. Niwa, *Appl. Catal. B: Environmen.* 40 (2003) 151–159. 15. K. Muto, N. Katada, M. Niwa, *Appl. Catal. B: Environmen.* 134 (1996) 203–215.
16. J.E. Mapes, R.P. Eischens, *J. Phys. Chem.* 78 (1954) 1059–62.
17. C. J. Van Oers, K. Góra-Marek, K. Sadowska, M. Mertens, V. Meynen, J. Datka, P. Cool, *Chem. Eng. J.* 237 (2014) 372–379.
18. J. Datka, M. Kawalek, K. Góra-Marek, *Appl. Catal. A*, 243 (2003) 293–299.
19. C. Lamberti, C. Prestipino, S. Bordiga, A.N. Fitch, G.L. Marra, *Nucl. Instr. Methods B.* 200 (2003) 155–159.
20. Y. Kim, K. Seff, *J. Am. Chem. Soc.* 99 (1977) 7055–7057.
21. Y. Kim, K. Seff, *J. Am. Chem. Soc.* 100 (1978) 6989–6997.
22. T. Sun, K. Seff, *Chem. Rev.*, 1994, 94 (4) 857–870.
23. S.G. Aspromonte, E.E. Miró, A.V. Boix, *Adsorption*, 18 (2012) 1–12.
24. H. Bernt, M. Richter, T. Gerlach, M. Baerns, *J. Chem. Soc., Faraday Trans.* 94 (1998) 2043–2046.

25. J. Shibata, K. Shimizu, Y. Takada, A. Shichi, H. Yoshida, S. Satokawa, A. Satsuma, T. Hattori, *J. Catal.* 227 (2004) 367–374.
26. A. Ausavasukhi, S. Suwannaran, J. Limtrakul, T. Sooknoi, *Appl. Catal. A*, 345 (2008) 89–96.
27. R. Bartolomeu, C. Henriques, P. Da Costa, F. Ribeiro, *Catal. Today* 176 (2011) 81–87.
28. A.M. Fonseca, I.C. Neves, *Microporous Mesoporous Mater.* 181 (2013) 83–87.
29. W.-S. Ju, M. Matsuoka, K. Iino, H. Yamashita, M. Anpo, *J. Phys. Chem. B* 108 (2004) 2128–2133.
30. A.M. Ferraria, A.P. Carapeto, A.M. Botelho do Rego, *Vacuum* 86 (2000) 1988–1991.
31. T.C. Kaspar, T. Droubay, S.A. Chambers, P.S. Bagus, *J. Phys. Chem. C* 114 (2010) 21562–21571.
32. H. Bernt, M. Richter, T. Gerlach, M. Baerns, *J. Chem. Soc., Faraday Trans.* 1998, 94, 2043–2046.
33. C. W. McDaniel and P. K. Maher, in *Molecular Sieves*, Society of Chemical Industry, London, UK, 1968, p. 186.
34. J.R. Sohn, S.J. Decanio, P.O. Fritz, J.H. Lunsford, *J. Phys. Chem.*, 1986.
35. R.D. Shannon, K.H. Gardner, R.H. Staley, G. Bergeret, P. Gallezot, A. Auroux, *J. Phys. Chem.* 89 (1985) 4778–4788.
36. A. Omega, J.A. van Bokhoven, R. Prins, *J. Phys. Chem. B*, 107 (2003) 8854–8860.
37. K. Tarach, K. Góra-Marek, M. Chrzan, S. Walas, *J. Phys. Chem. C*, 118 (2014) 23751–23760.
38. T. Pieplu, F. Pognant, A. Vallet, J. Saussey, J.-C. Lavalley, *Stud. Surf. Sci. Catal.*, 96 (1995), 619–626.
39. K. Hadjiivanov, *Microporous Mesoporous Mater.* 24, 1–3, (1998) 41–49.
40. L. Gang, L. Zhang, C. Zhang, H. He, *J. Catal.*, 261 (2009) 101–109.



265x198mm (150 x 150 DPI)